A Response Surface Methodology Based on Improved Compactly Supported Radial Basis Function and Its Application to Rapid Optimizations of Electromagnetic Devices

S. L. Ho[1], S. Y. Yang[1,2], G. Z. Ni[2], and H. C. Wong[3]

[1]Department of Electrical Engineering, Hong Kong Polytechnic University, Hong Kong
[2]College of Electrical Engineering, Zhejiang University, Zhejiang, China
[3]Industrial Center, Hong Kong Polytechnic University, Hong Kong

The compactly supported radial basis function (CS-RBF) is improved and used to design a new response surface model. The model is incorporated into stochastic global optimal methods to develop a fast and efficient global optimal design strategy with the main target to reduce the number of function calls that involve computationally heavy procedures such as, for example, the repetitive usage of finite element analysis which is generally required in solving inverse problems. In order to employ a multistep method to automatically adjust the support of the CS-RBF to realize the "best" tradeoff between computational efficiency and accuracy, a cluster algorithm is proposed to decompose the sample points into a nested sequence of subsets. To validate the proposed algorithm, typical numerical results on two different examples are reported.

***Index Terms*—Compact support, optimal design, radial basis function, response surface methodology.**

I. Introduction

DESIGN problems in electrical engineering usually involve elaborate and sophisticated computer simulations, involving typically computationally heavy procedures such as the repetitive usages of finite-element (FE) analysis in finding solutions of electromagnetic fields. Also, due to the multimodal and ill-conditioned natures of objective/constraint functions, the incorporation of global optimizers such as simulated annealing, genetic, evolutionary, tabu search, and particle swarm optimization methods into the computer simulation algorithm are inevitable. Compared to their deterministic counterpart methods, it is well known that a serious drawback of all the aforementioned stochastic optimal algorithms is their heavy computation burdens, i.e., at least thousands of iterations are generally required. The heavy computational burdens with these computer simulations often make the stochastic optimal methods impractical or impossible in the study of some practical design problems that require computationally heavy procedures. However, the preclusive use of stochastic optimal methods in the computer simulations for some design problems will inevitably degrade the quality of the final solutions. Thus, to reduce the number of function calls involving computationally heavy procedures such as the time-consuming FE simulations without sacrificing the accuracy of the numerical solutions, increasing efforts have recently been given to the developments of response surface models or methodologies (RSM) and their applications in the development of rapid global optimizations of electromagnetic devices in the study of computational electromagnetics [1]–[7].

Mathematically, a response surface model is an interpolation technique that fits a multidimensional function to its function values at some finite sample points on an arbitrary function domain. By using this technique, one will first discrete the decision variables into a set of sample points and then compute the function values at these points by using numerically heavy techniques such as finite-element analysis. The optimal problem is then reconstructed by using the selected response surface model and solved efficiently. The important point to note in this process is that the reconstructed RSM will calculate the objective and constraint functions swiftly and efficiently. Consequently, some computationally heavy design problems in electrical engineering that could not be solved hitherto can now be solved by means of these new techniques.

During the past two decades, the globally supported radial basis functions (RBFs) have undergone intensive researches and enjoyed considerable successes as a technique for multivariate interpolation of both scattered and grid data [8]–[10]. Unlike other interpolating functions, RBFs are not restricted to problems with only uniform data spacing. Due to their excellent interpolating performances, the globally supported RBFs are widely used in computational electromagnetics for reconstructing RSMs. However, although the RSMs based on global RBFs serve as very simple means to fit functions sampled at scattered data points in an arbitrary dimension, they inevitably suffer from a drawback of requiring a full interpolation matrix which is associated with all global interpolation methods, because the interpolated value is influenced by the complete set of data. On the other hand, in view of the approximation behavior, it is obvious that a higher density of sample points should yield a better approximation and hence it will be desirable to have as many sample points as possible. The evaluation of the reconstructed function will then be

Digital Object Identifier 10.1109/TMAG.2005.848610

dependent on a large number of points and is therefore very computationally expensive. The resulting condition number of the interpolation matrix is also very large, sometimes leading to numerical singularity of the interpolation matrix [9]. To circumvent the drawbacks associated with the application of globally supported RBFs in the function fitting, the multilevel method [11], the RBF modification of Shepard's method [12], and the CS-RBFs [13], among others, are potentially worthy of further studies. Moreover, the CS-RBF approach is the simplest one in numerical implementations.

On the other hand, to make the best use of the function values of the limited number of sample points, the sample points should be distributed in the feasible parameter space in an irregular pattern so that the point densities are higher in regions where the local optima are likely to exist. This kind of irregular sample distributions renders the use of CS-RBFs with a fixed support radius or seize infeasible, as the finding of the right scale becomes very awkward and difficult.

In this paper, the CS-RBF is improved and used to design a RSM for constructing computationally heavy objective or constraints functions because of its simplicity in numerical implementation, as well as because of its efficiency and accuracy in interpolations. To automatically adapt the support seize (scale parameter) of the CS-RBFs according to the densities of the sample points, a cluster algorithm to decompose the sample points into a nested sequence of subsets, together with the multilevel method, is proposed. The flexibility, accuracy, robustness, and the merits as well as disadvantages of the proposed method are elucidated by numerical results reported in this paper.

II. A CS-RBF Based RSM

A. Radial Basis Function Interpolation

Although RBFs are extensively used in recent years in computational electromagnetics, there is still a lack of a general introduction in both terminology and mathematical consistency. Let $R^+ = \{x \in R, x \geq 0\}$ and suppose a scale function $H : R^+ \rightarrow R$ be a continuous function with $H(0) \geq 0$. A radial basis function on R^d is a function defined in the form

$$H(\|X\|) \tag{1}$$

where $X \in R^d, \|\cdot\|$ is the Euclidean norm.

In general, the reconstruction of an objective or constraint function $f(X) : R^d \rightarrow R$ on the basis of its values f_i at a set of sample points $X_i \in R^d (i = 1, 2, \cdots, N)$ in terms of some radial basis function H is

$$f(x) = \sum_{j=1}^{N} c_j H(\|X - X_j\|). \tag{2}$$

The coefficients c_j are determined from the following matrix equation:

$$[c_j] = [H_{ij}]^{-1}[f_i] \tag{3}$$

where $H_{ij} = H(\|X_i - X_j\|)$ is called the interpolation matrix.

Clearly, to guarantee that (3) is solvable, the interpolation matrix H must be invertible. A sufficient condition for the interpolation matrix to be invertible is that the basis functions $H(\|X - X_j\|)$ is positive definite on R^d. Unfortunately, not all globally supported RBFs satisfy this condition, thus some polynomials should generally be added to (2) for a mathematically consistent implementation [14], although the interpolation form of (2) is commonly used by fellow researchers in the computational electromagnetics community.

As described previously, the main drawback associated with the use of globally supported RBFs is that the interpolation matrix is full. Due to their inefficiency in dealing with a full matrix, the sample points of the available RSMs could not exceed an upper limit of, for example, a few thousands such as 2500 as mentioned in [15]. Although this upper iteration limit is also the limit of the repetitive usages of FE analysis in general for inverse problems, this limit hinders the wide application of globally supported RBF based RSMs in electrical engineering. Moreover, when the spacing between sample points is very small, the interpolation matrix will become very ill-conditioned, leading to serious numerical singularity and degradation in the numerical accuracy. To overcome these problems, the CS-RBFs are improved and used in this paper.

The pioneering work about CS-RBFs is attributed to Wu [16], and its generalization reported by Wendland [13] in the mid-1990s. These functions of CS-RBF are strictly positive definite in R^n for all values of n less than or equal to some fixed value d and can be constructed with any desired degree of smoothness $2k$. The family of CS-RBFs constructed by Wendland [13] is used in this paper, since for a specific space dimension d, these functions posses the lowest positive degree among all piecewise polynomial compactly supported radial functions which are positive definite on R^d having a given order of smoothness. Generally, a CS-RBFs is expressed in the form

$$H_{d,k}(r) \doteq (1 - r)_+^n p(r) \quad (k \geq 0) \tag{4}$$

where $p(r)$ is a prescribed polynomial, $r = \| X \|, \doteq$ denotes equality up to a constant factor. For example

$$(1 - r)_+^n = \begin{cases} (1 - r)^n & (0 \leq r \leq 1) \\ 0 & (1 \geq r) \end{cases}. \tag{5}$$

The details about the CS-RBFs on an arbitrary dimension R^d are referred to in [13]. It should be pointed out that a function which is positive definite in R^d is also positive definite in R^k $(k < d)$. It should also be emphasized that the interpolation of CS-RBFs can be implemented in a simple way as formulated in (2) without any additional polynomial term due to their positive infinite property.

B. A RSM Based on Improved CS-RBFs

As demonstrated in [17], although the interpolation of the objective/constraint function using (2) performs very well in the inner region of the parameter space, it will give rise to significant errors in the derivatives on the boundary. To solve this problem, the information of the derivatives on the boundary of the parameter space is incorporated into (2), and the interpolation becomes

$$f(X) = \sum_{j=1}^{N} c_j H(\|X - X_j\|) + \sum_{k=1}^{N_B} d_k H'(\|X - X_j\|) \tag{6}$$

where N is the number of the total sample points, and N_B is the number of the boundary sample points used only for derivative fitting.

The coefficients c_j and d_k are determined from the following matrix equation:

$$\begin{bmatrix} c_j \\ d_k \end{bmatrix} = \begin{bmatrix} H_{11} & H_{12} \\ H_{21} & H_{22} \end{bmatrix}^{-1} \begin{bmatrix} f_j \\ f'_k \end{bmatrix} \tag{7}$$

where

$$\begin{aligned} (H_{11})_{ij} &= H(\|X_i - X_j\|) \quad (i,j = 1,2,\ldots,N) \\ (H_{12})_{ij} &= H'(\|X_i - X_j\|) \\ &\qquad (i = 1,2,\ldots,N; j = 1,2,\ldots,N_B) \\ (H_{21})_{ij} &= H'(\|X_i - X_j\|) \\ &\qquad (j = 1,2,\ldots,N; i = 1,2,\ldots,N_B) \\ (H_{22})_{ij} &= H''(\|X_i - X_j\|) \quad (i,j = 1,2,\ldots,N_B). \end{aligned} \tag{8}$$

Due to the compactly supported nature of the proposed RBFs, the interpolation matrix H is sparse. Thus, the addition or removal of some sample points causes only a local change in the interpolation results. Further research shows that the performances of the RBFs as formulated in (4) is often overshadowed in many practical engineering design problems that have large dimensions in which the objective/constraint functions have significant differences in the "curvatures" of directions of different decision variables. To address this issue in real engineering problems, an improved CS-RBF with the introduction of curvature parameters is proposed. Mathematically, the high-dimensional RBFs being proposed is defined as

$$H_j(r) = H\left(\sqrt{\sum_{i=1}^{d}((x_i - (x_i)_j) \Big/ D_i)^2}\right) \tag{9}$$

where d is the dimension of the decision parameters, D_i is a curvature parameter which controls the "curvature" of the reconstructed function in the ith direction at the point X_j.

Furthermore, to guarantee good numerical performances for the solution of (7), the sample points on the boundary for fitting function values should generally be different from those for fitting function derivatives. Thus, the density of the sample points in the boundaries should be higher than that of the inner regions in their neighborhoods. In numerical implementation, some of these boundary points are used for fitting function values, while the others are used for fitting derivatives.

C. A Cluster Algorithm to Decompose the Sample Points Into a Nested Sequence of Subsets

As explained in the introduction, to make the best use of the function values of the limited number of sample points, the sample points should be distributed in the feasible parameter space in an irregular pattern such that the point densities are higher in regions where the local optima are likely to exist. Thus, every CS-RBF should have the ability to adjust its support according to the point density around it. Correspondingly, the CS-RBFs are of the form $H(\cdot/\alpha)$ for $\alpha > 0$ (α will be called the scale parameter hereafter). When deciding the scale parameter of a CS-RBF, one must keep in mind that: 1) if the scale is too low, the interpolation will be very poor and 2) on the other hand, if the scale is too large, the interpolation matrix is no longer sparse enough to make its inversion efficient, and this is indeed the main reason for choosing CS-RBFs.

Therefore, a reasonable selection of the scale parameter is the best tradeoff of the accuracy and efficiency of the interpolation. Consequently, a multistep method as proposed in [18] is used in this paper. The multistep method is a hierarchical method which uses M interpolation levels based on a nested sequence decomposition of subsets of the sample points. For the convenience of understanding the cluster algorithm as proposed in this paper, one shall recap the multistep methods as described in the following paragraphs.

Let $X = \{X_1, X_2, \ldots, X_N\}$ be a set of sample points in a domain $D \in R^d$ with the corresponding function values $f_i (i = 1,2,\ldots,N)$. One shall first decompose the set X into a nested sequence

$$X^1 \subset X^2 \subset \cdots X^{M-1} \subset X^M = X \tag{10}$$

of the subset X_k of X

$$X^k = \left\{X_1^{(k)}, X_2^{(k)}, \ldots, X_{N_k}^{(k)}\right\} \quad (1 \le k \le M) \tag{11}$$

and the interpolation problem is decomposed into M steps by the following steps.

Starting with $k = 1$, at the kth step one matches the error function

$$f - (s^1 + s^2 + \cdots s^{k-1}) \tag{12}$$

on X_k by computing the coefficients of the kth interpolant

$$\begin{aligned} s_k(Y) = &\sum_{j=1}^{N_k} c_j^k H\left(\left\|Y - X_j^{(k)}\right\| \Big/ \alpha_k\right) \\ &+ \sum_{j=1}^{N_k^B} d_j^k H'\left(\left\|Y - X_j^{(k)}\right\| \Big/ \alpha_k\right) \end{aligned} \tag{13}$$

after the scale α_k of the basis function has been chosen.

It follows naturally that

$$f|_X = (s^1 + s^2 + \cdots + s^M)|_X. \tag{14}$$

This approach allows one to choose a relatively large scale at the lowest level to capture the overall behavior of the function, and by decreasing it during the process of the procedure, finer and finer details of the function is obtained step by step, providing a hierarchical construction procedure with an acceptable computing time. In other words, this approach allows one to adjust the support of the CS-RBFs according to the point density, with a reasonable tradeoff between interpolation efficiency and accuracy, that would still result in an improvement in the interpolation quality. Thus, one needs to decompose the sample points into a nested sequence of subsets. For this purpose, a cluster algorithm is proposed.

First, the parameter space is divided into a discrete grid according to a user predefined precision parameter. The discrete grid is recorded as a binary string. When a sample point is generated, its location in the grid is determined by repeatedly bisecting the range of it in each direction and to identify the specific half range that contains the solution. The corresponding

bit of the strings is then set to a logical 1. Once the total sample points, X, are generated and the binary string is assigned, the maximum distances, $d_i^{\max}(i = 1, 2, \ldots, d)$, among every two neighborhood points for each coordinate direction, will be evaluated and the algorithm will begin to decompose the sample points X into a nested sequence of subsets, $X^1 \subset X^2 \subset \cdots X^{M-1} \subset X^M = X$, by using the following algorithm.

Cluster Algorithm: Generation of the first subset X^1. Use the point of the first nonzero logical 1 in the left bottom of the hyper-box as a vertex and taking $d_i^{\max}$ as the edge length of the ith direction; construct a hyper-box; Propagate from the vertexes of this hyper-box, construct, one by one, the defined hyper-boxes until the nonzero logical 1s of the grid are covered by the vertexes of the hyper-boxes; The subset X^1 is then consisting of the vertex points of the total hyper-boxes whose values in the binary string are logical 1s; Set the bits of the binary string corresponding to points in X^1 to logical 2s;

Repeat

$X^i = X^{i-1}$;

Step 1. Halve the edge length of the hyper-boxes of the previous step to construct new hyper-boxes, find logical 1s of the vertex points, add the corresponding points to X^i and set the bit values of the binary string to logical 2s;

Step 2. Let $X^{\mathrm{dif}} = X^i - X^{i-1}$. If the number of sample points in X^{dif} is less than a threshold value prescribed by the user, go to Step1; otherwise, continue the decomposing process for next level;

Until all the bits of the binary string are equal to logical 2s or 0s.

III. A Fast Optimal Strategy Based on Combinations of the Proposed CS-RBF and Stochastic Methods

To accelerate the speed of stochastic optimal algorithms for solving computationally heavy design problems, a strategy based on the combination of the improved CS-RBF based RSM and stochastic algorithms is proposed and is described as:

Initialization: Generate a number of sample points; Compute the objective/constraint function values using computationally heavy algorithms such as FE analysis at these sample points; determine the value of the derivatives of the objective/constraint functions on the boundary sample points. Decompose the sample points into a nested sequence of subsets;

Step 1: Reconstruct the optimal problem using the multistep method based on the proposed CS-RBF based RSM;

Step 2: Solve the reconstructed optimal problem by a stochastic method, then report all the searched local/global optimal solutions;

Step 3: Solve the original optimal problem by using a deterministic method starting from the newly searched local optimal solutions to find the final ones.

As explained previously, to make the best use of the function values of the limited number of sample points, the sample points should be distributed in the feasible parameter space in an irregular pattern such that the point densities are higher in regions where the local optima are likely to exist. To this end, different adaptive approaches to add nodes in the optimization process are proposed by fellow researchers [2], [7]. In this paper, a relatively simple simulated annealing algorithm is proposed to run first on the computationally heavy optimal problem to generate the sample points because the simulated annealing algorithm has some "intelligence" in generating new points, i.e., intensifying points in regions where the local optima exist. Of course, when the number of the total sample points is of the order of a few hundreds, a well engineered simulated annealing algorithm is unlikely to step into the stage of generating sampling points "intelligently." In such cases, one should deliberately design a "less-well" engineered simulated annealing algorithm by setting a relatively small control parameter (temperature) in the process of generating sample points.

IV. Numerical Examples

A. Validation

A mathematical function as formulated in (15) is deliberately designed with a significant difference in the "curvatures" among different variable directions to elucidate the interpolation power of the proposed RSM using the improved CS-RBFs. Specifically

$$f(x, y) = e^{-x}\sin(4x)e^{-y}\sin(30y) \quad (0 \le x, y \le 1). \tag{15}$$

For comparative purpose, this mathematical function is reconstructed by using three different response surface models, i.e., the proposed CS-RBF based one, the proposed CS-RBF based one with the scale parameter D_i as defined in (9) being deliberately precluded, and a globally supported RBF based one. The CS-RBF used in this paper is

$$H(r) = (1 - r)_+^4(4 + 16r + 12r^2 + 3r^3) \tag{16}$$

and the globally supported RBF used is

$$h(r) = (r^2 + 0.1)^{0.04}. \tag{17}$$

To reconstruct this mathematical function, the simulated annealing algorithm is first used to generate 495 sampling points for fitting the function values, and 11 equidistance sampling points in each boundary are used for fitting derivatives on the boundary, resulting in a total number of 535 sample points. The distribution of these 535 sample points in the feasible decision variable space is depicted in Fig. 1. The mathematical function is then reconstructed by using the aforementioned three RSMs, respectively. To evaluate the performances of different RSMs, the following deviances are used:

$$\text{Deviance-A } (DA) = \sum_{i=1}^{N} (f_i^{\mathrm{ex}} - f_i^{\mathrm{com}})^2 \tag{18}$$

$$\text{Deviance-B } (DB) = \sum_{i=1}^{N} |f_i^{\mathrm{ex}} - f_i^{\mathrm{com}}| \tag{19}$$

where f_i^{ex} and f_i^{com} are, respectively, the close-form solution and the predicated value of the test function at sample point i by using a RSM; N is the number of observing points.

In the evaluation, 41 equidistance sampling points along each coordinate direction (a total of 1681 observing points) are used as observing points to calculate theses deviances, and the corresponding numerical results of the deviances of the reconstructed functions from the close-form expression are given in Table I. Moreover, for illustration purposes, the reconstructed functions

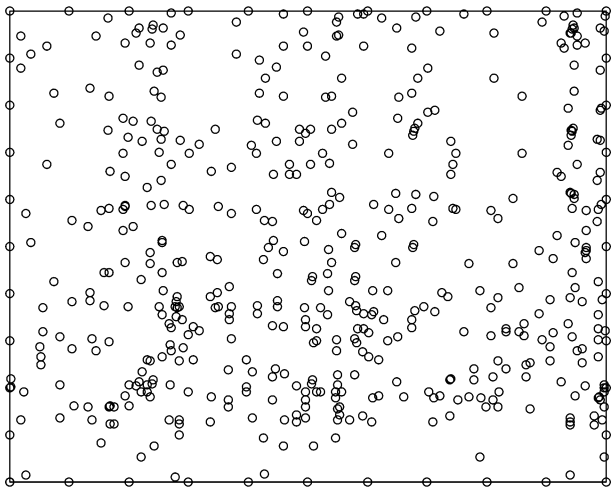

Fig. 1. Distribution of the 535 sample points for the mathematical test function.

TABLE I
DEVIANCE COMPARISON OF DIFFERENT RSMS FOR THE TEST FUNCTION

	Proposed RSM	Proposed RSM without scale	The globally supported RBF
DA	0.1258	1.4944	0. 1184
DB	10.6960	36.3676	10.4242

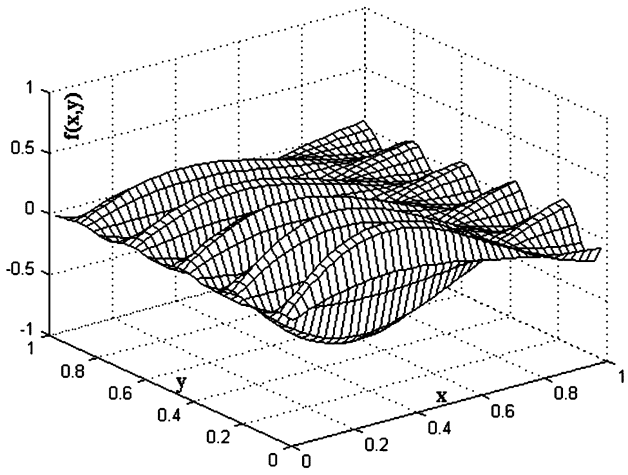

Fig. 2. Reconstructed mathematical function using the proposed RSM.

using different RSMs as well as the close-form expression are shown in Figs. 2–5.

From these numerical results, it is clear, at least for this test function, that:

1) Introducing a scale parameter into the CS-RBF based RSM will significantly improve the performance of the RSM model when the reconstructed function has significant "curvatures" in different coordinate directions.
2) The performances of the proposed CS-RBF based RSM are comparable to those of the specific globally supported RBF based one but the computational efficiency of the former is much higher than that of the later when the number of simple points is large.
3) In addition to attractive performances in terms of deviances (numerical accuracies), the proposed RSM is also very robust in producing the stationary points (local/global optima) as demonstrated by the figures. This merit is the most important feature when applying RSM to solve a practical engineering design problem.

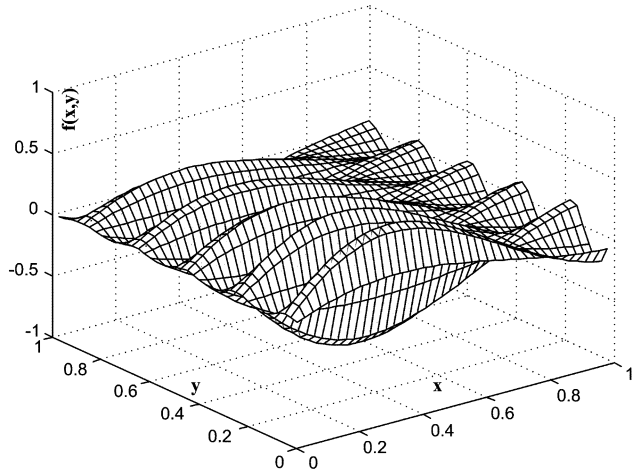

Fig. 3. Reconstructed mathematical function using the proposed RSM with the scale parameter being deliberately precluded.

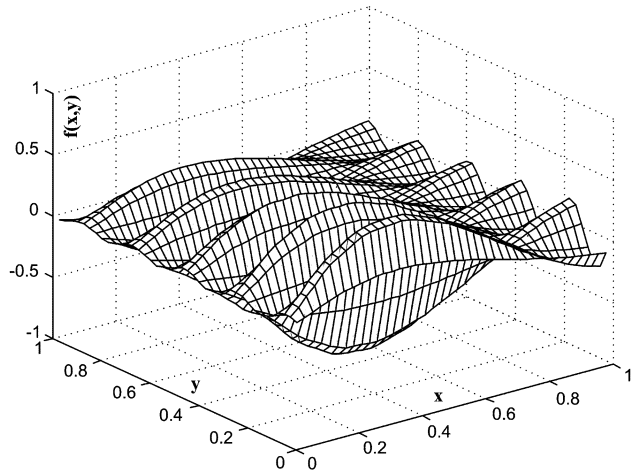

Fig. 4. Reconstructed mathematical function using the specific globally supported RBF.

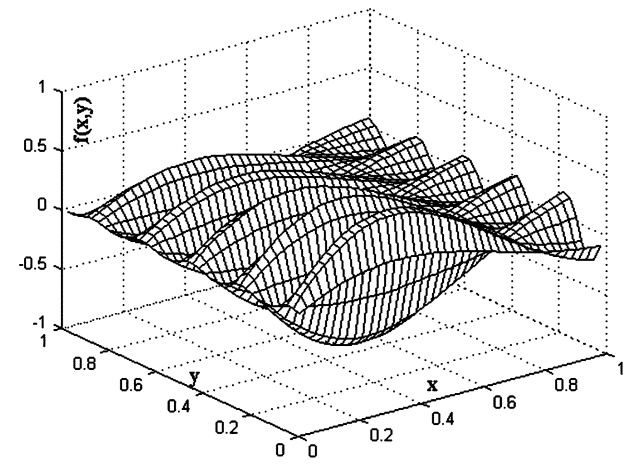

Fig. 5. Illustration of the close-form mathematical function.

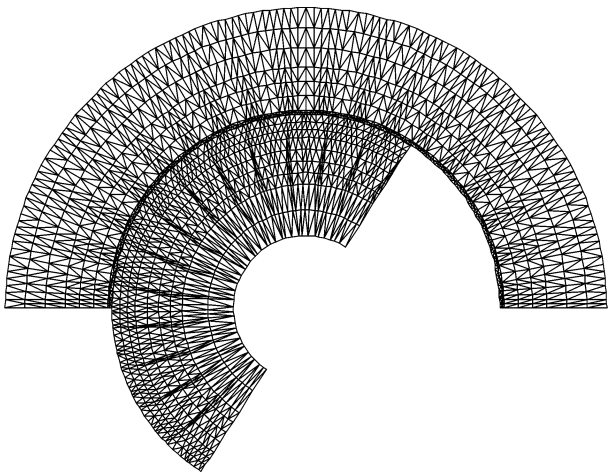

Fig. 6. Mesh used for finite-element analysis.

B. Case Study

To test the feasibility of the proposed fast optimal strategy in solving computationally heavy design (inverse) problems, the torque ripple minimization problem of a prototype squirrel cage induction motor drive fed from a PWM inverter at rated operating conditions as reported in [19] is selected as the case study. Mathematically, this optimal problem is formulated as

$$\begin{aligned} &\min f = \frac{1}{T_0}\sqrt{\sum_{i=0}^{N_f} T_i^2(\alpha)} \\ &\text{s.t. } \alpha_{i-1} + \Delta_{\min} \le \alpha_i \le \alpha_{i+1} - \Delta_{\min} (i = 2, \ldots, N) \\ &\quad \alpha_1 \ge \alpha_{\min}, \quad \alpha_N \le \alpha_{\max} \end{aligned} \tag{20}$$

where N is the number of switching angles within one quarter period of the PWM inverter; α_i is the ith switching angle; T_i is the ith component of the electromagnetic torque; $\Delta_{\min}, \alpha_{\min}$, and $\alpha_{\max}$ are related to the switching frequency of the power electronic elements and the operating conditions.

To consider the nonlinear property of the magnetic materials and the relative movement between the stator and the rotor, the iterative procedure based on a time-stepping (complex) FE method coupled with the external circuit model of [19] is used to compute the steady state electromagnetic fields and the performance criteria.

As outlined in the previous section, in the numerical implementation of the proposed strategy, the following steps are executed.

1) The simulated annealing algorithm is first used to generate 1200 sample points in the feasible regions of decision variables in such a way that the points are densely populated around the local optimal points. Moreover, 68 sample points which are uniformly distributed on the boundaries for derivative fitting are also desired. The corresponding objective/constraint function (including derivatives of those boundary points) values are determined using the computationally heavy approach of the time-stepping (complex) FE method coupled with the external circuit model. The mesh used in the FE analysis is given in Fig. 6.
2) The optimal problem is then reconstructed using the proposed CS-RBF based RSM and solved by using a tabu search algorithm to find the "nearly" optimal solution. The improved tabu search method as proposed by the authors is used in this phase, and the details about the algorithm are referred to in [20]. The CS-RBF used in this step is a positive definite one with 4 smoothness (C^4) on R^5, and is defined as

$$H(r) = (1-r)_+^7(16r^2 + 7r + 1). \tag{21}$$

The iterative number used by the tabu search method on the reconstructed optimal problem is 9052.
3) Finally, a simplex method is run directly on the original computationally heavy design problem by starting from these searched "nearly" optimal solutions to find the final optimal solution.

TABLE II
PERFORMANCE COMPARISON OF THE PROPOSED AND TRADITIONAL APPROACHES FOR THE CASE STUDY

	α_1(deg)	α_2(deg)	α_3(deg)	α_4(deg)	α_5(deg)	f	No FEM computation
Tabu	5.18	18.06	19.89	33.69	34.98	1.01	7862
Proposed	5.19	18.07	20.01	33.70	35.12	1.009	1268+46*

*46 is the iterative number used by the simplex method.

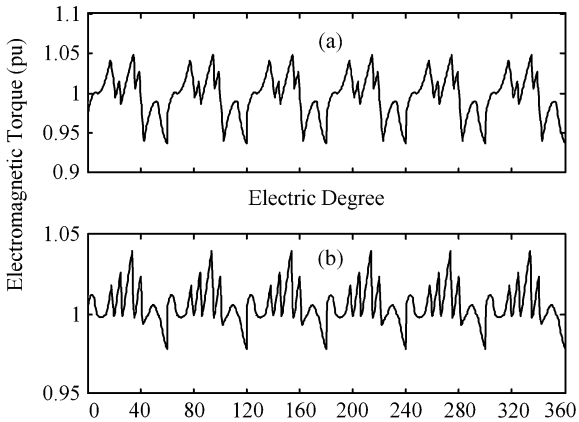

Fig. 7. Steady-state electromagnetic torques. (a) and (b) are, respectively, the torque before and after the optimization of the proposed strategy.

For the performance comparison, this problem is also solved directly by using a traditional strategy, i.e., the computationally optimal problem is directly solved by the tabu search method. The final optimal solutions of a prototype PWM inverter-fed motor with six switching angles within one quarter period of the PWM inverter obtained by different methods, together with their performance comparison, are given in Table II. The profiles of the electromagnetic torques and phase currents of the stator before and after the optimizations are shown in Figs. 7 and 8, respectively.

From these numerical results, it is obvious that:

1) the final optimal results obtained by the two different optimal approaches are nearly the same;
2) the number of the FE analysis of the proposed method is less than one fifth of that needed by the chosen stochastic optimal method commonly used by fellow researchers;
3) an additional searching process of the improved tabu method is required on the reconstructed optimal problem for the proposed rapid optimal strategy to reach the final solutions, resulting in an iterative cycle with 9052 iterations.

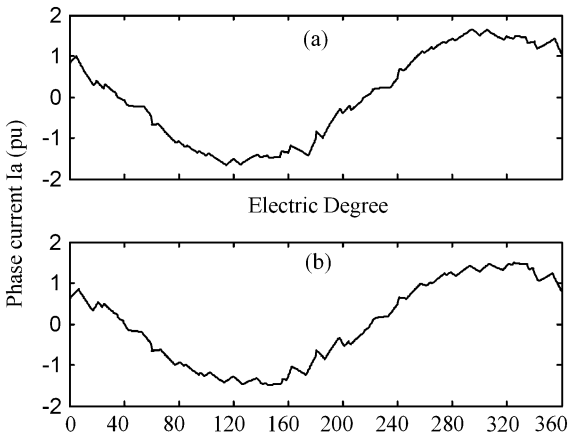

Fig. 8. Stator current profiles of the machine. (a) and (b) are, respectively, the torque before and after the optimization of the proposed strategy.

However, since the CPU time for a function call on the reconstructed problem is negligible compared to that of a function call in which the FE simulation is involved, the enhancement of the computational efficiency of the proposed optimal scheme is significant. Therefore, these numerical results confirm that the proposed approach is very efficient in solving optimal problems in which the objective/constraint function must be determined by means of computationally heavy approaches such as the 3-D FE analysis. In short, the proposed work provides a reliable alternative for fast and efficient optimizations of complex engineering design problems.

V. Conclusion

A new response surface methodology based on an improved compactly supported radial basis function which gives the available RBFs a reasonable compromise on computation efficiency and accuracy is proposed. When the CS-RBF is combined with stochastic global optimal methods, an efficient and accurate global optimizer is realized. The issues associated with its numerical implementation such as the adaptive regulation of the scale parameter of the CS-RBFs are also fully addressed. By way of comparison and testing, the accuracy, efficiency, and the advantages of the proposed algorithm for solving engineering inverse problems is positively confirmed.

Acknowledgment

This work was supported by the Research Grant Council of the Hong Kong Special Administrative Region, China, under Project PolyU 5242/04E.

References

[1] D. N. Dyck and D. A. Lower, "Response surface modeling of magnetic device performance using function value and gradient," *Int. J. Appl. Electromagn. Mach.*, vol. 9, pp. 241–248, 1998.

[2] M. Farina and J. K. Sykulski, "Comparative study of evolution strategies combined with approximation techniques for practical electromagnetic optimization problems," *IEEE Trans. Magn.*, vol. 3237, no. 5, pp. 3216–3220, Sep. 2001.

[3] K. Rashid, M. Farina, J. A. Ramirez, J. K. Sykulski, and E. M. Freeman, "A comparison of two generalized response surface methods for optimization in electromagnetics," *COMPEL*, vol. 20, pp. 740–752, 2001.

[4] T. Ishikawa, Y. Tsuke, and M. Matsunami, "A combined method for global optimization using radial basis function and deterministic approach," *IEEE Trans. Magn.*, vol. 35, no. 3, pp. 1730–1733, May 1999.

[5] Z. Malik and K. Rashid, "Comparison of optimization by response surface methodology with neurofuzzy methods," *IEEE Trans. Magn.*, vol. 36, no. 1, pp. 241–257, Jan. 2000.

[6] F. Gillon and P. Brochet, "Screening and response surface method applied to the numerical optimization of electromagnetic devices," *IEEE Trans. Magn.*, vol. 36, no. 4, pp. 1163–1167, Jul. 2000.

[7] M. C. Costa, J.-L. Coulomb, Y. Marechal, A. B. Dietrich, and S. I. Nabeta, "Diffuse-element method and quadtrees: Two "ingredients" for an adaptive response surface," *IEEE Trans. Magn.*, vol. 38, no. 2, pp. 1085–1088, Mar. 2002.

[8] N. Dyn, "Interpolation of scattered data by radial functions," in *Approximation Theory VI*, C. K. Chui, L. L. Schumaker, and J. D. Ward, Eds. New York: Academic, 1989, vol. 1, pp. 211–234.

[9] D. Lazzaro and L. B. Montefusco, "Radial basis functions for multivariate interpolation of large scattered data sets," *J. Comput. Appl. Math.*, vol. 140, pp. 521–536, 2002.

[10] R. Schaback, "Creating surface from scattered data using radial basis functions," in *Mathematical Methods for Curves and Surfaces*, M. Daehlen, T. Lyche, and L. L. Schumaker, Eds. Nashville, TN: Vanderbilt Univ. Press, 1989, pp. 477–496.

[11] M. S. Floater and A. Iske, "Multistep scattered data interpolation using compactly supported radial basis functions," *J. Comput. Appl. Math.*, vol. 73, pp. 65–78, 1995.

[12] D. Lazzaro and L. B. Montefusco, "Radial basis functions for the multivariate interpolation of lager scattered data sets," *J. Comput. Appl. Math.*, vol. 140, pp. 521–536, 2002.

[13] H. Wendland, "Piecewise polynominal, positive definite and compactly supported radial functions of minimal degree," *Adv. Comput. Math.*, vol. 4, pp. 389–396, 1995.

[14] M. A. Golberg, C. S. Chen, and H. Bowman, "Some recent results and proposals for the use of radial basis functions in the BEM," *Eng. Anal. Boundary Elements*, vol. 23, pp. 285–296, 1999.

[15] P. Alotto, A. Bertoni, and M. Nervi, "An efficient hybrid algorithm for the optimization of problems with several local minima," *Int. J. Numer. Meth. Eng.*, vol. 50, pp. 847–868, 2001.

[16] Z. Wu, "Multivariate compactly supported positive definite radial functions," *Adv. Comput. Math.*, vol. 4, pp. 283–292, 1995.

[17] X. Zhang, K. Z. Song, and X. Liu, "Meshless methods based on collocation with radial basis functions," *Comput. Mech.*, vol. 26, pp. 333–343, 2000.

[18] M. S. Floater and A. Iske, "Multistep scattered data interpolation using compactly supported radial functions," *J. Comput. Appl. Math.*, vol. 73, pp. 65–78, 1996.

[19] S. L. Ho, S. Y. Yang, P. Zhou, H. C. Wong, and M. A. Rahman, "A combined finite element-domain elimination method for minimizing torque ripples in inverter-fed ac drive systems," *IEEE Trans. Magn.*, vol. 36, no. 4, pp. 1817–1821, Jul. 2000.

[20] S. L. Ho, S. Y. Yang, G. Z. Ni, and H. C. Wong, "An improved tabu search for global optimizations of electromagnetic devices," *IEEE Trans. Magn.*, vol. 37, no. 5, pp. 3570–3574, Nov. 2001.

Manuscript received October 7, 2003, revised March 28, 2005.